Propagation characteristics of auroral kilometric radiation observed by the MEMO experiment on Interball 2

Michel Parrot, François Lefeuvre, Jean-Louis Rauch, Ondřej Santolík, M.M. Mogilevski

JOURNAL OF GEOPHYSICAL RESEARCH, VOL. 106, NO. A1, PAGES 315-325, JANUARY 1, 2001

Propagation characteristics of auroral kilometric radiation observed by the MEMO experiment on Interball 2

M. Parrot, F. Lefeuvre, and J. L. Rauch

Laboratoire de Physique et Chimie de l'Environnement, Centre National de la Recherche Scientifique Orléans, France

O. Santolìk

Faculty of Mathematics and Physics, Charles University, Prague

M. M. Mogilevski

Space Research Institute, Russian Academy of Sciences, Moscow

Abstract. The MEMO experiment is a part of the Interball 2 wave consortium. It is connected to a total of six electric and nine magnetic independent sensors. It provides waveforms associated with the measurement of two to five components in the three frequency bands: ELF (5-1000 Hz), VLF (1-20 kHz), and LF (20-250 kHz). Waveforms of three magnetic components and one electric component recorded during observations of auroral kilometric radiation (AKR) allow a detailed study of the characteristics of these emissions. In particular, the wave normal directions of AKR relative to the Earth's magnetic field are determined using several methods: the classical methods based on the plane wave approximation [*Means*, 1972] and the wave distribution function method which represents the evaluation of the wave energy density distribution with respect to the angular frequency and the wave normal direction(s). One event is fully analyzed in this paper. It is shown that AKR propagates with a polarization quasi-circular (ellipticity value ~ 0.9), a right polarization (i.e., R-X mode), and wave normals weakly oblique (~ 30°).

1. Introduction

This paper deals with the determination of wave normal directions in the frequency fine structure of auroral kilometric radiation (AKR) observed on the Interball 2 satellite. It is based on the simultaneous measurements of the three magnetic wave field components and of one electric field component. It completes a preliminary paper from *Lefeuvre et al.* [1998] where analyses of Interball 2 data were based on the plane wave hypothesis.

Several wave analysis techniques have been used to determine the wave normal directions of auroral kilometric radiations. The first measurements of the propagation characteristics were obtained by using occultations of the emission by the moon [*Alexander and Kaiser*, 1976; *Kaiser and Alexander*, 1976]. Under the assumption of a purely transverse electromagnetic wave, estimates of the direction have been derived from the spin-null method, that is, from the modulation of the signal associated with the measurement of one electric field component [*Gurnett*, 1974; *Kurth et al.*, 1975; *Kaiser and Stone*, 1975; *Kaiser et al.*, 1978; *James*, 1980; *Mellot et al.*, 1984; *Calvert and Hashimoto*, 1990; *Hilgers et al.*, 1992a]. A more precise estimation, based on the change of the relative phase of the signals received by two orthogonal antennas during a spin revolution, has been proposed by *Calvert* [1985]. It has also been used by *Mellott et al.* [1985, 1986] and *Huff et al.* [1988]. Now all these methods assume that the observed wave behaves as a plane wave. Moreover, they have a weak time resolution (the spin period at least) and depend on the relative positions of the spin axis, the Earth's magnetic field direction, and the wave vector.

The situation is much better when one measures a larger number of field components. *Morioka et al.* [1990] used five-component measurement of the Akebono satellite to calculate the Poynting flux vector in the satellite frame. With onboard narrow-band receivers they studied phase relations between the field components in a band of 100 Hz inside an AKR emission. The Interball 2 satellite also allows the measurement of several components. The computation by the POLRAD experiment [*Hanasz et al.*, 1998] of the nine Stokes parameters of the three electric wave field components allows the full determination of the wave normal directions in a fraction of a second. The only hypothesis that

Paper number 2000JA900072.
0148-0227/01/2000JA900072$09.00

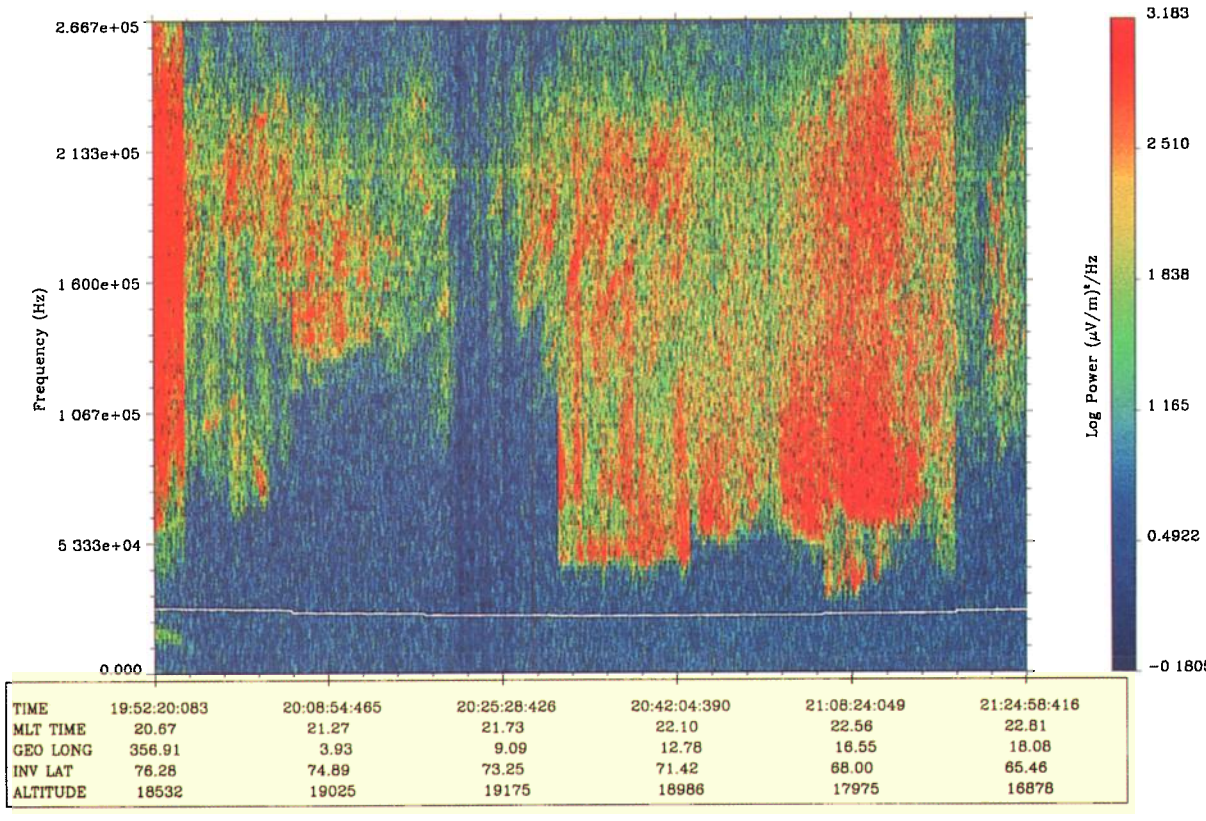

Plate 1. AKR event recorded by MEMO on January 28, 1997, with an electric sensor. The spectrogram starts at 1952:20 UT and ends at 2124:58 UT. The other parameters are the magnetic local time, the geographic longitude, the invariant latitude, and the altitude of the satellite. It must be noted that regular gaps without data have been suppressed in order to produce a continuous plot. Read 2.667e+05 as 2.667×10^5.

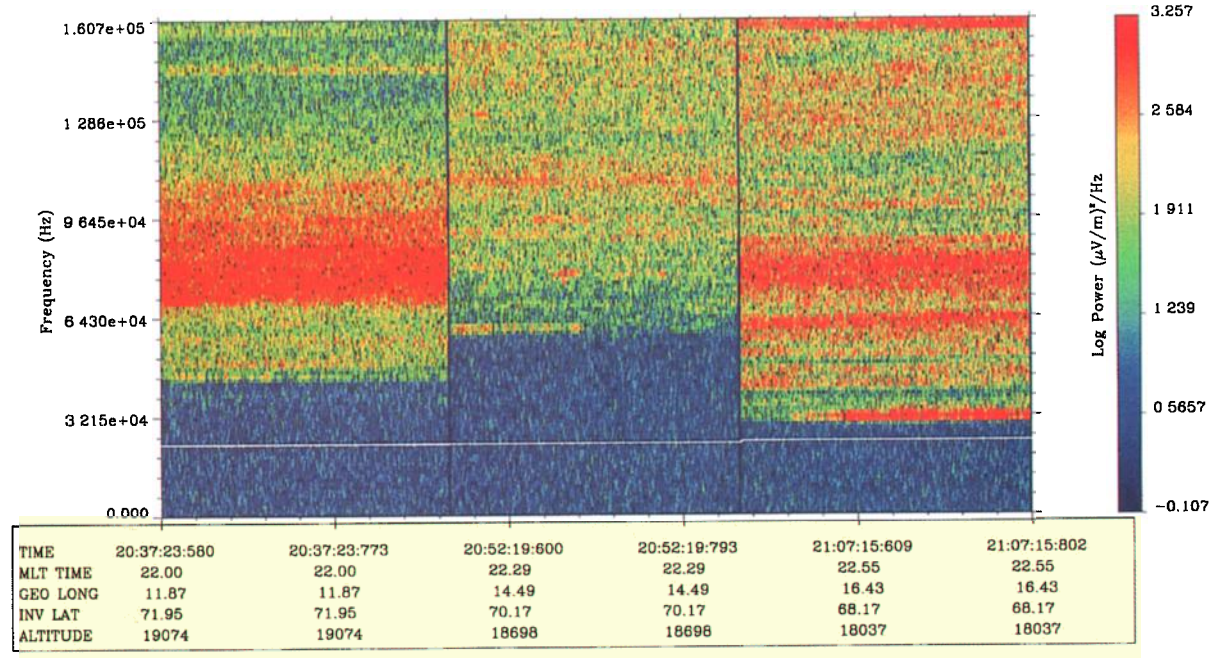

Plate 2. Spectrogram representation of three bursts extracted from the event of Plate 1 at 2037:23, 2052:19, and 2107:15. The duration of each burst is 0.32 s, and the frequency is limited to 160 kHz. The parameters displayed below are identical to those in Plate 1. Read 1.607e+05 as 1.607×10^5.

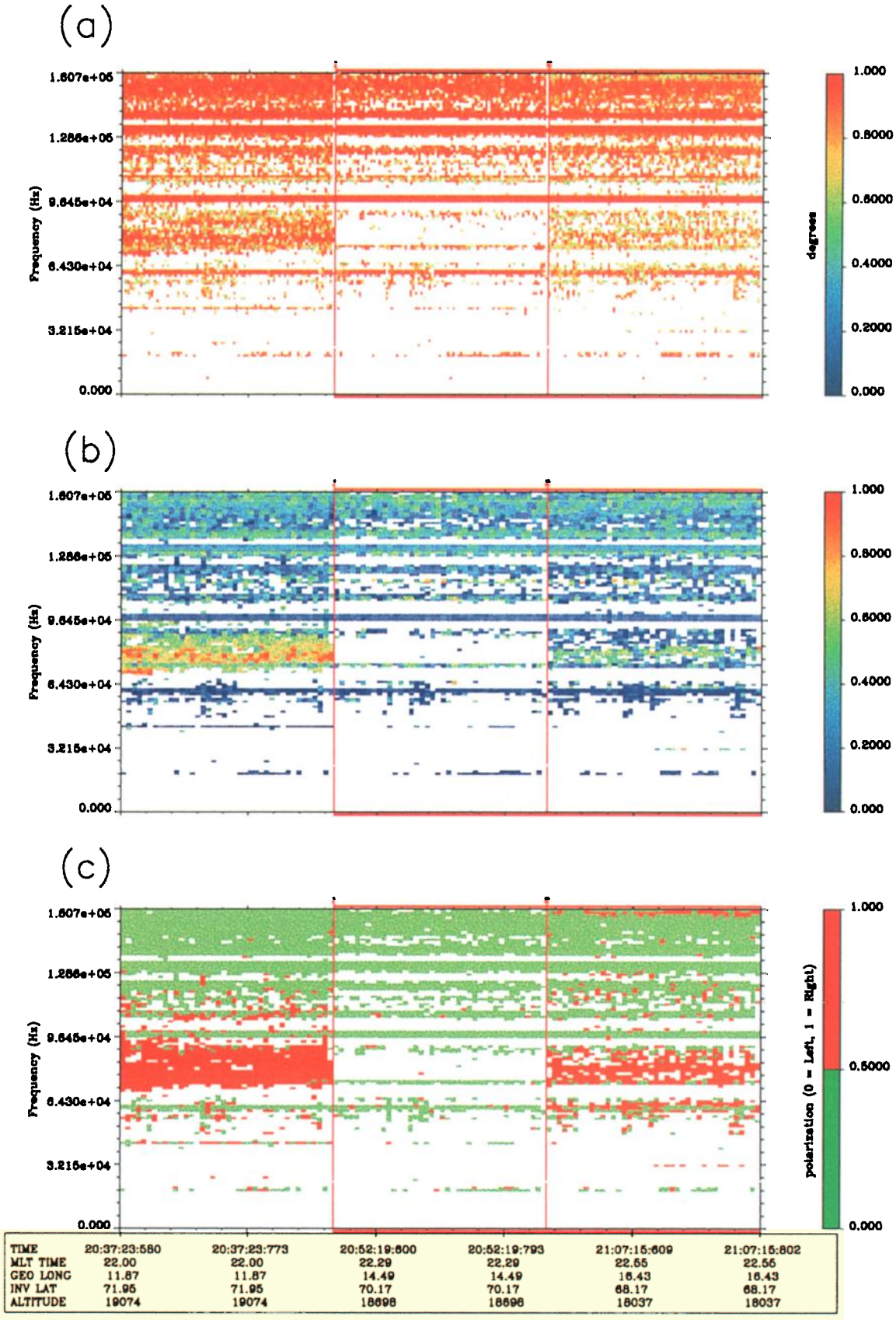

Plate 3. For the data shown in Plate 2: (a) a spectrogram representing the degree of polarization, (b) a spectrogram representing the wave ellipticity, and (c) a spectrogram representing the sense of polarization. Read 1.607e+05 as 1.607×10^5.

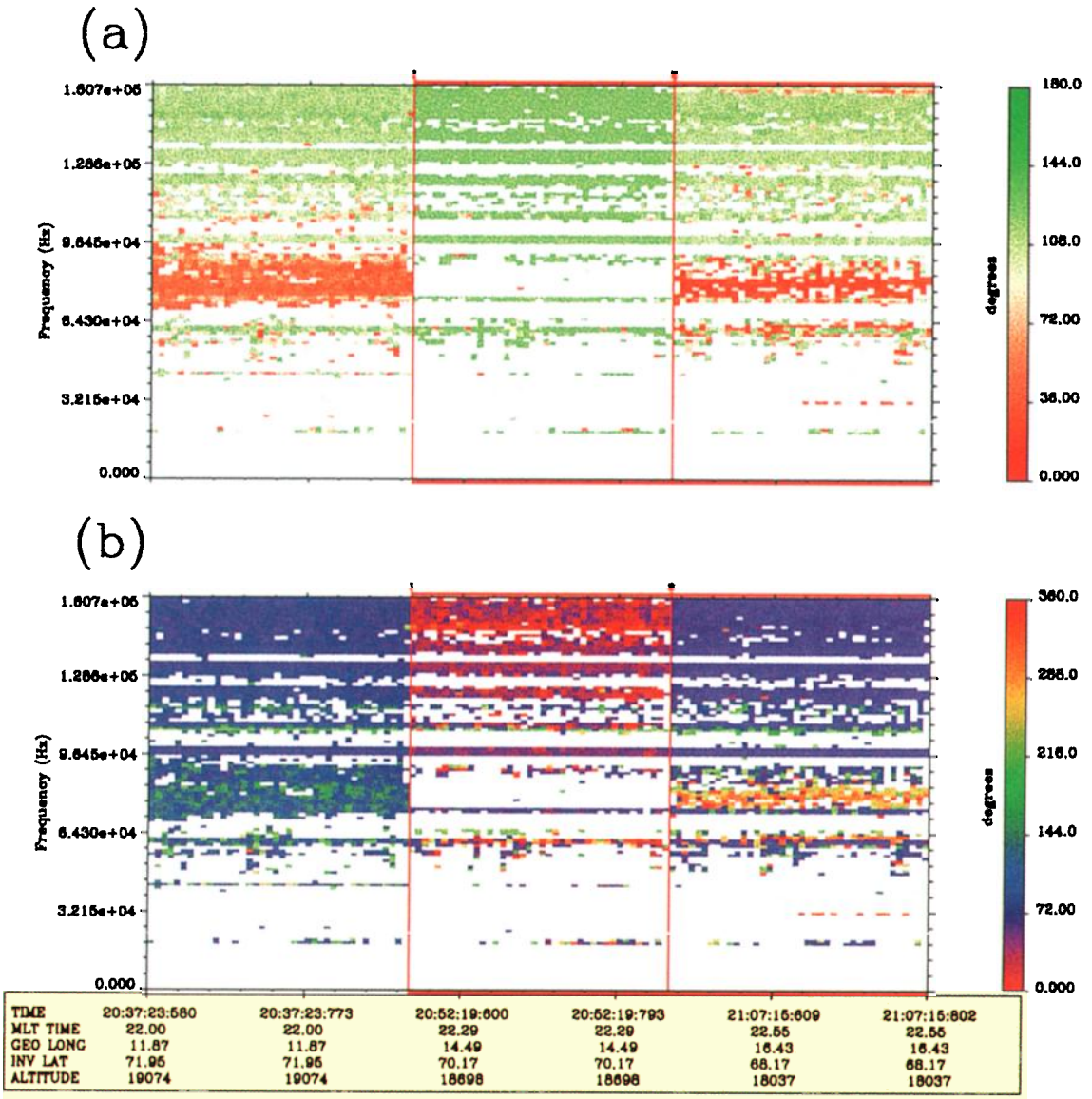

Plate 4. For the data shown in Plate 2: (a) a spectrogram representing the θ angle, and (b) a spectrogram representing the φ angle. The angle values are displayed according to the color scale on the right.

has to be made is that the wave is a plane wave. The transmission to the ground by the MEMO experiment [*Lefeuvre et al.*, 1998] of the waveforms of four wave field components (one electric and three magnetic) give still greater facilities. In their publication on preliminary results, Lefeuvre et al. have shown how classical methods of direction findings could be used to determine the wave normal direction under the plane wave hypothesis. But such an hypothesis is not compulsory. It is the objective of the present paper to show how the plane wave hypothesis may be tested and how non plane waves may be analyzed.

The use of high-resolution methods is particularly needed to analyze AKR temporal fine structures, lasting a few seconds or less, which have been pointed out by numerous authors [*Gurnett et al.*, 1979; *Gurnett and Anderson*, 1981; *Benson et al.*, 1988]. They are associated with particle acceleration structures [*de Feraudy et al.*, 1988; *Louarn et al.*, 1990; *Ungstrup et al.*, 1990; *Hilgers et al.*, 1991, 1992b; *Pottelette et al.*, 1992]. On the other hand, fine, narrow bandwidth, drifting structures (<1 kHz), with rapidly varying center frequencies, have been observed [*Gurnett et al.*, 1979; *Gurnett and Anderson*, 1981; *Morioka et al.*, 1981; *Baumback and Calvert*, 1987; *Benson et al.*, 1988]. However, most theories proposed for AKR assume that the plasma is homogeneous and do not take into account the existence of fine structures. Observations have been explained in terms of a movement of the AKR source region along magnetic field lines [*Gurnett et al.*, 1979; *Gurnett and Anderson*, 1981]. Maser emissions in non-uniform magnetic fields have been studied [*Le Quéau et al.*, 1985; *Zarka et al.*, 1986; *Le Quéau and Louarn*, 1989]. A nonlinear theory of radiation from the interaction between lower hybrid solitons and upper hybrid waves has been developed [*Pottelette et al.*, 1992]. But none of the proposed interpretations has been confirmed. Non-ambiguous determinations of the polarization characteristics within these structures and measurements of the phase relationships between different frequency bands may provide key parameters for the generation mechanisms.

Section 2 will present the wave analysis methods we used to determine the propagation characteristics of AKR. The analysis of an AKR event is presented in section 3, whereas discussion and conclusions are given in section 4.

2. Wave Analysis Methods

Various methods are used to determine wave characteristics in this study. The wave normal direction of the waves is calculated when the magnetic component frame is transformed in an orthogonal frame of reference linked to the Earth's magnetic field B_0: the z axis lies along B_0, the x axis points toward the direction of decreasing magnetic latitude in the local magnetic meridian plane, and the y axis completes the orthogonal set. In this system the wave normal direction $\mathbf{k}$ is characterized by the polar angle θ and the azimuthal angle φ. Three independent plane wave methods are used to determine the $\mathbf{k}$ direction (only one is used in this paper). They give correct values only when the plane wave approximation is valid. We used the method of *Means* [1972] which is based on the imaginary part of the spectral matrix. The determination of the sense of polarization for quasi-parallel waves is based on the sign of the imaginary part of the cross spectrum between the x and y components [*Lefeuvre et al.*, 1986]. If this sign is positive, the waves are right-hand polarized; if it is negative, the waves are left-hand polarized. The degree of polarization is directly estimated from the spectral matrix of the three magnetic components. Under the plane wave hypothesis the ellipticity is estimated from the eigenvector associated with the non null eigenvalue in the plane wave hypothesis [*Samson and Olson*, 1980].

When the assumption of a plane wave is not valid, the determination of the wave distribution function (WDF) is required. The WDF specifies the distribution of wave energy density with respect to the frequency and the wave normal direction [*Storey and Lefeuvre*, 1974, 1979, 1980]. Examples of wave analysis with WDF are given by *Lefeuvre and Delannoy* [1979], *Parrot and Lefeuvre* [1986], and *Lefeuvre et al.* [1992]. For the WDF treatment we need to know the plasma frequency and the electron gyrofrequency.

For the Means' method the WDF is able to remove the ambiguity of the direction of wave propagation (in the direction of B_0 or opposite) when at least one electric component is used. But this electric component and the magnetic components must be in the same frame of reference [see, e.g., *Santolik and Parrot*, 1999].

3. Propagation Characteristics of an AKR Event

3.1. Data

The MEMO experiment is a part of the wave experiment consortium onboard the satellite Interball 2 which was launched into an elliptical orbit on September 6, 1996, with an inclination of 65 degrees, an apogee altitude of 19,200 km, and a perigee altitude of 772 km. A full description of the experiment is given by *Lefeuvre et al.* [1998]. MEMO is connected to a total of six electric and nine magnetic sensors working in three different frequency ranges: ELF (5-1000 Hz), VLF (1-20 kHz), and LF (20-250 kHz). There are two operating modes: a survey mode with low-resolution data in order to provide an overview of the measured wave phenomena, and a burst mode where the waveforms of the three magnetic components and one electric component are recorded for short time intervals. The spectrogram in the bottom panel of Plate 1 represents one AKR event recorded by MEMO on January 28, 1997, using the survey mode. It shows data from an electric component in the LF range up to 266.7 kHz for a period of nearly 1 hour and 30 min. The intensity is color coded according to the scale on the right and the geophysical parameters are given at the bottom. It is a night pass at high invariant latitude (65°-76°) around the satellite apogee. Fine, narrow bandwidth, drifting structures appear from 100 up to 250 kHz. Strong AKR emissions with a low-frequency part down to ~ 40 kHz can be observed at the beginning, and between 2029 and 2123 UT. During this former time interval, three snapshots of data have been

recorded in the burst mode, and their spectrograms are given in Plate 2. The three spectrograms are recorded at 2037:23, 2052:19, and 2107:15, respectively, and their duration is 0.32 s. For the analysis they are limited in frequency to 160 kHz because the data for the magnetic components are corrupted by interference at higher frequencies. The middle spectrogram does not display any particular features because there is a small gap in AKR activity. In the first panel a large AKR frequency band is seen between 70 and 100 kHz, whereas in the third panel, temporal fine structures are found to occur at frequencies starting as low as 32 kHz. The emissions below the white line which represents the electron gyrofrequency have no meaning due to the low-frequency cutoff of the MEMO HF filter.

3.2. Propagation Characteristics

3.2.1. Plane wave analysis. The analysis described in section 2 has been applied to the magnetic data which correspond to the spectrograms shown in Plate 2. Time-frequency plots of different parameters are collected in Plate 3. Plate 3a shows the degree of polarization. From this plot we can get information for a given frequency and time similarly as in the spectrogram of Plate 2. According to the color scale on the right, the degree of polarization is coded between blue (0) and red (1). White represents the regions of low signal intensity where the magnetic power-spectral density is lower than 4×10^{-4} mγ^2/Hz. We see in the first panel that the emission observed around 80 kHz tends to have a high degree of polarization. The emissions of highest intensity are generally well polarized with a polarization degree larger than 0.75 except at 32 kHz in the third panel. This low polarization degree indicates that the assumption of a single plane wave is certainly not valid in this case.

The ellipticity of the wave polarization is given in Plate 3b and coded between blue (linear polarization) and red (circular polarization). In the first panel the ellipticity around 80 kHz is often between 0.75 and 1, which indicates that the polarization is practically circular, whereas in other cases nothing can be said when the degree of polarization is low. For example, in the third panel the emissions at 32 and 159 kHz have an ellipticity value around 0.5 which indicates a non well-determined polarization.

Information about the wave polarization is extended in Plate 3c. The sense of polarization in the plane perpendicular to B_0 is indicated by red or green spots. It is obviously undefined when the polarization is linear. Plate 3c indicates that the more intense emissions (the large band emission in the first panel and the fine structures in the third panel) are right-hand polarized.

The wave normal directions are given in Plates 4a and 4b where the two angles θ and φ are represented according to the color scale on the right, respectively. They are obtained with the Means' method. Plate 4a indicates that waves around 80 kHz in the first and the third panel have practically the same θ values (~35°), whereas it is seen in Plate 4b that the angles φ are different in the two panels and separated approximately by 180°.

3.2.2. WDF analysis. Since we have found that the plane wave hypothesis is not valid in the spectrograms shown in Plate 2, we have done a more detailed analysis of the AKR propagation at various frequencies using the WDF method. The amount of data recorded during the bursts represented in Plate 2 allows several different analyses, and the first and the third data intervals in Plate 2 have been divided into 10 parts. For all the events, the electron gyrofrequency is ~23.5 kHz. Without a reliable determination of the plasma frequency we have taken a value of 11 kHz at 2037 UT and a value of 8.5 kHz at 2107 UT. As the estimation mainly relies on the magnetic components, the results are not sensitive to a multiplication by 0.5 or 2. The assumption of a *R-X* mode and a cold plasma are used in this analysis. Plate 5 shows the results of the WDF analysis performed at the beginning and end of the first burst of data in Plate 2 at time intervals 1 and 10. Four analyses have been made at a frequency of 80 kHz and each is represented by two polar plots. For example, the first plot on the left in the first row is related to waves propagating in the direction of the magnetic field, whereas the second plot in the first row is related to the same analysis but for waves propagating in direction opposite to the magnetic field. Each plot displays the intensity of the WDF in arbitrary units as a function of the azimuthal angle θ and the polar angle φ. In these two plots and the two others on the same row it is impossible to distinguish between upgoing and downgoing waves because only the three magnetic components have been used. It is observed that the maximum of the WDF is centered on θ = ~30° and φ = ~300°. The energy is not well localized because there is some extension of the WDF maximum in θ and φ. It is noticed that the analysis performed on the last part (part 10) of the time interval of the same burst shows similar features concerning the direction and the extension of the WDF. The second row concerns the WDF analysis when we take in addition one electric component. It allows the separation between upgoing and downgoing waves. It is seen that the waves are in the opposite direction of the magnetic field and therefore upgoing as is expected in the Northern Hemisphere where the magnetic field is directed toward the Earth. For the third burst of data, WDF analysis can be performed at different frequencies when the emissions are strong, and Plate 6 displays these results. Three time intervals have been selected (part 4, 7, and 10) and three frequencies (32.1, 80.7, and 159.2 kHz). The three magnetic plus one electric components are used. Several important points can be observed:

1. For all the time intervals the WDFs are almost identical at a given frequency.

2. Moreover, they are identical during all the time intervals of the burst at the two frequencies 32.1 and 80.7 kHz.

3. The azimuthal angle θ is nearly identical to the value observed in the first burst 30 min before.

4. From the first burst to the third the angle φ changes. This angle is shifted by ~180° (this is underlined in Plate 7 where two WDFs analysis at 80 kHz separated by a time interval of 30 min are represented).

5. The WDF at 159.2 kHz presents features which are different from the analysis at other frequencies which seems

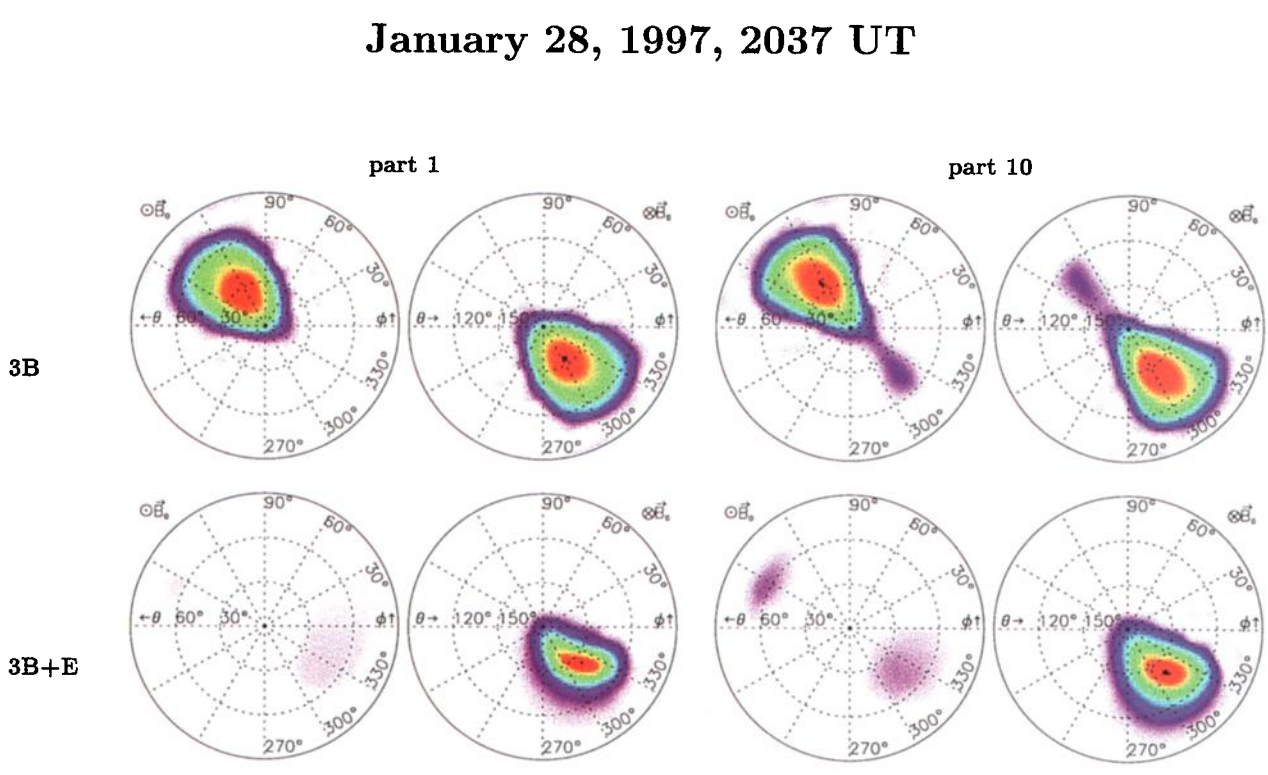

Plate 5. WDF analysis for the first burst of Plate 2 at a frequency equal to 80 kHz (see text for explanation), January 28, 1997, 2037 UT.

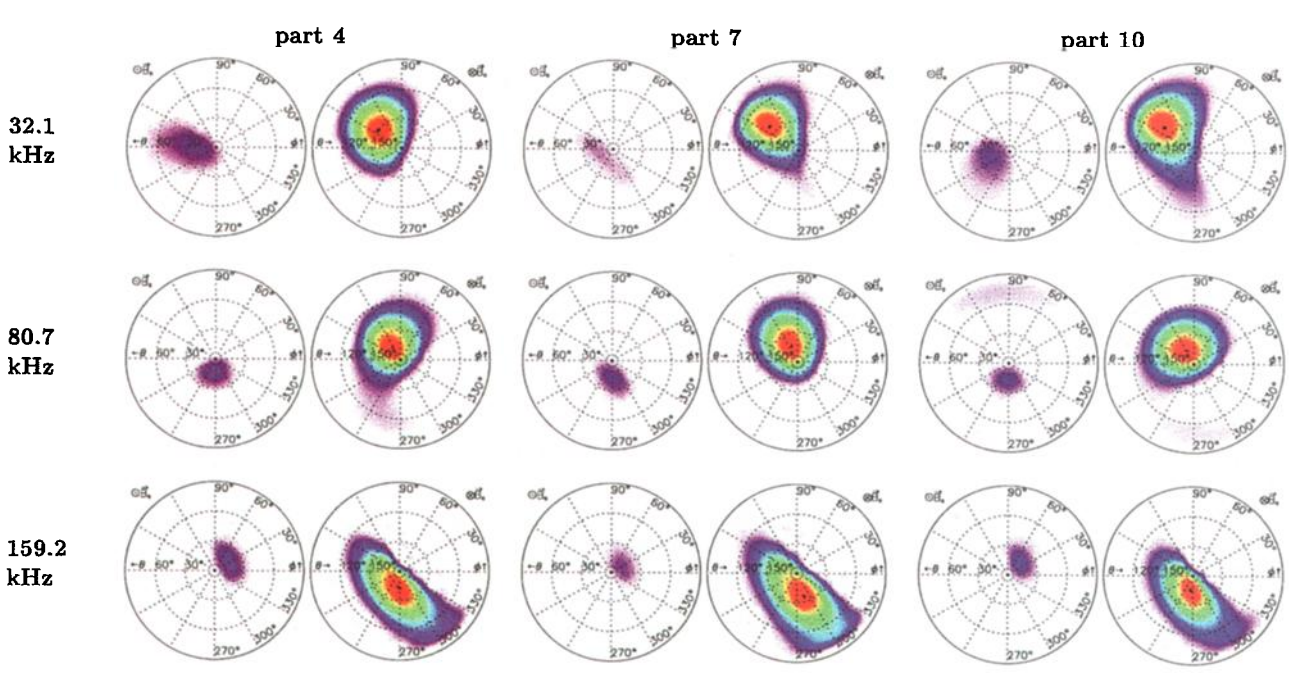

Plate 6. WDF analysis for the third burst of Plate 2 at three different frequencies (32.1, 80.7, and 159.2 kHz), January 28, 1997, 2107 UT.

January 28, 1997, 80 kHz

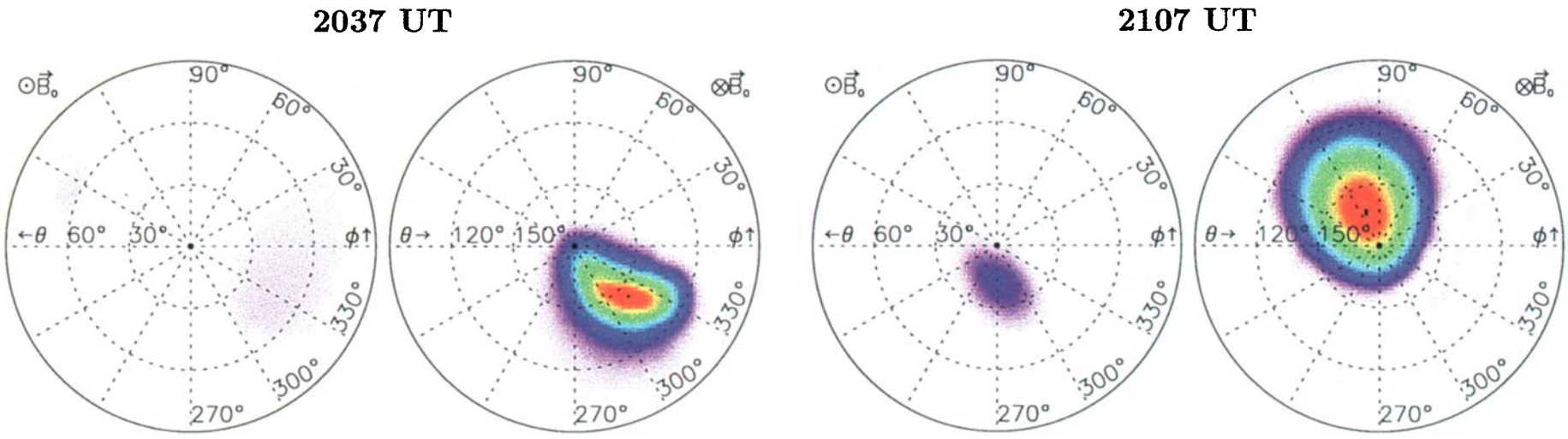

Plate 7. Two WDFs analyses at the same frequency for the data of the first burst and the third burst, respectively, on January 28, 1997, 80 kHz.

Table 1. Transfer Function of the Electric Component Estimated by the WDF Method at Three Different Frequencies.

	32,142 Hz		80,729 Hz		159,220 Hz	
Step	Amplitude	Phase, deg.	Amplitude	Phase, deg.	Amplitude	Phase, deg.
0	8.231	-35.946	7.995	-70.939	8.099	-41.268
1	2.824	123.318	7.866	-74.436	8.251	-35.946
2	5.547	10.565	7.734	-66.000	8.231	-35.373
3	7.545	5.541	7.525	-71.112	8.199	-34.334
4	7.955	18.242	8.241	-69.974	8.262	-34.223
5	8.917	16.002	7.264	-75.638	7.335	-41.653
6	7.938	21.327	7.585	-68.502	8.486	-41.926
7	8.999	15.293	8.347	-70.546	8.271	-34.227
8	10.364	14.864	8.039	-67.356	8.225	-29.214
9	8.345	21.734	7.717	-71.083	8.231	-35.946

to indicate that this emission may have a different origin.

It must be noted that the use of an electric component is subject to caution. Due to the unknown coupling impedance between the antenna and the plasma, it is impossible to correctly evaluate the cross spectra between the electric and magnetic components. In the analysis shown before, we have considered the coupling impedance (the phase shift and amplitude change) of the antenna output with respect to the wave electric field as an unknown parameter. We have estimated the WDF together with this parameter, but it is a dangerous process because in fact we change the amplitude of the electric component. Then we have checked the estimation on several parts of the signal considering that there is no change in the plasma during 0.32 s. The results are shown in Table 1. It concerns the 10 parts of data of the third burst at three different frequencies (32.1, 80.7, and 159.2 kHz). For each frequency the estimated phase and amplitude are given. It is observed that for a given frequency the estimated amplitude and phase are roughly similar in all 10 parts of the signal. This is not true at 32 kHz for the first parts of the time interval because the signal is low (see Plate 2), and then the estimation is not meaningful.

4. Discussion and Conclusions

This paper describes the first accurate determination of AKR wave normal direction. Because of the high altitude of Interball 2, this AKR event is obviously observed from above the AKR source region. At the altitude of the observations, AKR propagates with a polarization that is quasi-circular and in the *R-X* mode. The wave normals are weakly oblique at a wave angle of 30°. It is observed that at a given frequency the characteristics of the emission are rather constant for a long time interval (30 min). The propagation characteristics are also similar for emissions which seems dissociated because they appear at different frequencies. This implies that in our event the discrete emissions observed at 32.1 and 80.7 kHz in the third burst probably have the same origin. The variation of φ between 2037 and 2107 UT also suggests that Interball 2 was just above the source region during this time interval.

Acknowledgments. Michel Blanc thanks Michael L. Kaiser and Wynne Calvert for their assistance in evaluating this paper.

References

Alexander, J.K., and M.L. Kaiser, Terrestrial kilometric radiation, 1, Spatial structure studies, *J. Geophys. Res., 81*, 5948, 1976.

Baumback, M.M., and W. Calvert, The minimum bandwiths of auroral kilometric radiation, *Geophys. Res. Lett., 14*, 119, 1987.

Benson, R.F., M.M. Mellott, R.L. Huff, and D.A. Gurnett, Ordinary mode auroral kilometric radiation fine structure observed by DE 1, *J. Geophys. Res., 93*, 7515, 1988.

Calvert, W., DE-1 measurements of AKR wave direction, *Geophys. Res. Lett., 12*, 381, 1985.

Calvert, W., and K. Hashimoto, The magnetosonic modes and

propagation properties of auroral kilometric radiation, *J. Geophys. Res.*, *95*, 3943, 1990.

de Feraudy, H., A. Bahnsen, and M. Jesperen, Observation of nightside and dayside auroral kilometric radiation with Viking, in *Proceedings of 2nd International Workshop on Radio Emission from Planetary Magnetosphere*, edited by H.O. Rucker, S.J. Bauer, and B.M. Pedersen, p. 239, Verlag der Österreichischen Akademie der Wissenschaften, Vienna, 1988.

Gurnett, D.A., The Earth as a radio source: Terrestrial kilometric radiation, *J. Geophys. Res.*, *79*, 4227, 1974.

Gurnett, D.A., and R.R. Anderson, The kilometric radio emission spectrum: Relationship to auroral acceleration processes, in *Physics of Auroral Arc Formation, Geophys. Monogr. Ser.*, vol. 25, edited by S.-I. Akasofu and J.R. Kan, p. 341, AGU, Washington, D.C., 1981.

Gurnett, D.A., R.R. Anderson, F.L. Scarf, R.W. Fredericks, and E.J. Smith, Initial results from the ISEE 1 and 2 plasma wave investigation, *Space Sci. Rev.*, *23*, 103, 1979.

Hanasz, J., R. Schreiber, H. de Feraudy, M.M. Mogilevsky, and T.V. Romantsova, Observations of the upper frequency cutoffs of the auroral kilometric radiation, *Ann. Geophys.*, *16*, 1097, 1998.

Hilgers, A., A. Roux, and R. Lundin, Characteristics of AKR sources: A statistical description, *Geophys. Res. Lett.*, *18*, 1493, 1991.

Hilgers, A., H. de Feraudy, and D. Le Quéau, Measurements of the *E* field polarization of AKR inside the sources, *J. Geophys. Res.*, *97*, 8381, 1992a.

Hilgers, A., B. Holback, G. Holmgren, and R. Boström, Probe measurements of low plasma densities with applications to the auroral acceleration region and auroral kilometric radiation sources, *J. Geophys. Res.*, *97*, 8631, 1992b.

Huff, R.L., W. Calvert, J.D. Craven, L.A. Frank, and D.A. Gurnett, Mapping of auroral kilometric radiation sources to the aurora, *J. Geophys. Res.*, *93*, 11,445, 1988.

James, H.G., Measurements of auroral kilometric radiation and associated VLF data from ISIS 1, *J. Geophys. Res.*, *85*, 3367, 1980.

Kaiser, M.L., and J.K. Alexander, Source location measurement of terrestrial kilometric radiation obtained from lunar orbit, *Geophys. Res. Lett.*, *3*, 37, 1976.

Kaiser, M.L., and R.G. Stone, Earth as an intense planetary radio source: Similarities to Jupiter and Saturn, *Science*, *189*, 285, 1975.

Kaiser, M.L., J.K. Alexander, A.C. Riddle, J.B. Pearce, and J.W. Warwick, Direct measurement by Voyager 1 and 2 of the polarization of terrestrial kilometric radiation, *Geophys. Res. Lett.*, *5*, 857, 1978.

Kurth, W.S., M.M. Baumback, and D.A. Gurnett, Direction findings measurement of auroral kilometric radiation, *J. Geophys. Res.*, *80*, 2764, 1975.

Lefeuvre, F., and C. Delannoy, Analysis of random electromagnetic wave field by a maximum entropy method, *Ann. Telecommun.*, *34*, 204, 1979.

Lefeuvre, F., Y. Marouan, M. Parrot, and J.L. Rauch, Rapid determination of the sense of polarization and the sense of propagation for random electromagnetic fields: Applications to GEOS 1 and AUREOL 3 data, *Ann. Geophys.*, *6*, 457, 1986. (Correction, *Ann. Geophys.*, *5A*(4), 252, 1987.)

Lefeuvre, F., J. L. Rauch, D. Lagoutte, J. J. Berthelier, and J. C. Cerisier, Propagation characteristics of dayside low-altitude hiss: Case studies, *J. Geophys. Res.*, *97*, 10,601, 1992.

Lefeuvre, F., M. Parrot, J.L. Rauch, B. Poirier, A. Masson, and M. Mogilevsky, Preliminary results from the MEMO multicomponent measurements of waves on-board Interball 2, *Ann. Geophys.*, *16*, 1117, 1998.

Le Quéau, D., and P. Louarn, Analytical study of the relativistic dispersion: Application to the generation of the AKR, *J. Geophys. Res.*, *94*, 2605, 1989.

Le Quéau, D., R. Pellat, and A. Roux, The maser synchrotron instability in an inhomogeneous medium: Application to the generation of auroral kilometric radiation, *Ann. Geophys.*, *3*, 273, 1985.

Louarn, P., A. Roux, H. de Feraudy, D. Le Quéau, M. André, and L. Matson, Trapped electrons as a free energy source for the auroral kilometric radiation, *J. Geophys. Res.*, *95*, 5983, 1990.

Means, J.D., Use of the three-dimensional covariance matrix in analyzing the polarization properties of plane waves, *J. Geophys. Res.*, *77*, 5551, 1972.

Mellot, M.M., W. Calvert, R.L. Huff, D.A. Gurnett, and S.D. Shawhan, DE 1 observations of ordinary mode and extraordinary mode auroral kilometric radiation, *Geophys. Res. Lett.*, *11*, 1188, 1984.

Mellot, M.M., R.L. Huff, and D.A. Gurnett, The auroral kilometric radiation: DE 1 direction finding studies, *Geophys. Res. Lett.*, *12*, 479, 1985.

Mellot, M.M., R.L. Huff, and D.A. Gurnett, DE 1 observations of harmonic auroral kilometric radiation, *J. Geophys. Res.*, *91*, 13,732, 1986.

Morioka, A., H. Oya, and S. Miyatake, Terrestrial kilometric radiation observed by the satellite Jikiken, *J. Geomagn. Geoelectr.*, *33*, 37, 1981.

Morioka, A., H. Oya, and K. Kobayashi, Polarization and mode identification of auroral kilometric radiation by PWS system onboard the Akebono (EXOS-D) satellite, *J. Geomagn. Geoelectr.*, *42*, 443, 1990.

Parrot, M., and F. Lefeuvre, Statistical study of the propagation characteristics of ELF hiss observed on GEOS-1, outside and inside the plasmasphere, *Ann. Geophys.*, *4*, 363, 1986.

Pottelette, R., R.A. Treumann, and N. Dubouloz, Auroral kilometric radiation generation from lower hybrid solitons upper hybrid waves interaction, *J. Geophys. Res.*, *97*, 12,029, 1992.

Samson, J.C., and J.V. Olson, Some comments on the descriptions of the polarization states of waves, *Geophys. J. R. Astron. Soc.*, *61*, 115, 1980.

Santolik, O., and M. Parrot, Case studies on the wave propagation and polarization of ELF emissions observed by Freja around the local proton gyrofrequency, *J. Geophys. Res.*, *104*, 2459, 1999.

Storey, L.R.O., and F. Lefeuvre, Theory for the interpretation of measurements of a random electromagnetic wave field in space, *Space Res.*, *14*, 381, 1974.

Storey, L.R.O., and F. Lefeuvre, The analysis of 6-component measurement of a random electromagnetic wave field in a magnetoplasma, 1, The direct problem, *Geophys. J. R. Astron. Soc.*, *56*, 255, 1979.

Storey, L.R.O., and F. Lefeuvre, The analysis of 6-component measurement of a random electromagnetic wave field in a magnetoplasma, 2, The integration kernels, *Geophys. J. R. Astron. Soc.*, *62*, 173, 1980.

Ungstrup, E., A. Bahnsen, J.K. Wong, M. André and L. Matson, Energy source and generation mechanism for auroral kilometric radiation, *J. Geophys. Res.*, *95*, 5973, 1990.

Zarka, P., D. Le Quéau, and F. Genova, The maser synchrotron instability in an inhomogeneous medium: Determination of the spectral intensity of auroral kilometric radiation, *J. Geophys. Res.*, *91*, 13,542, 1986.

F. Lefeuvre, M. Parrot, and J.L. Rauch, Laboratoire de Physique et Chimie de l'Environnement, CNRS, 3A, Avenue de la Recherche Scientifique, 45071 Orléans Cedex 02, France. (lefeuvre@cnrs-orleans.fr; mparrot@cnrs-orleans.fr; jlrauch@cnrs-orleans.fr)

M.M. Mogilevski, IKI, Russian Academy of Sciences, 117081 Moscow, Russia. (mogilevsky@romance.iki.rssi.ru)

O. Santolìk, KEVF-MFF, Faculty of Mathematics and Physics, Charles University, V Holesovickach 2, 18000 Praha 8, Czech Republic. (ondrej.santolik@mff.cuni.cz)

(Received February 16, 2000; revised March 27, 2000; accepted April 28, 2000.)